*M&C 2017 - International Conference on Mathematics & Computational Methods Applied to Nuclear Science & Engineering, Jeju, Korea, April 16-20, 2017, on USB (2017)*

# Uncertainty Quantification of Bell Factor for Sjöstrand Method using Random Sampling Method

Toshiki Kimura, Tomohiro Endo, Akio Yamamoto

*Nagoya University: Furo-cho, Chikusa-ku, Nagoya, Japan, 464-8603*
*t-kimura@fermi.nucl.nagoya-u.ac.jp, t-endo@nucl.nagoya-u.ac.jp, a-yamamoto@nucl.nagoya-u.ac.jp*

**Abstract** – *Sjostrand Method is one of the subcriticality measurement techniques for the accelerator driven system (ADS). In this study, we investigated the uncertainty quantification of a spatial correction factor, Bell factor, due to cross-section data, using the random sampling method. As a result, the uncertainty of the Bell factor due to cross-section uncertainty is smaller than that of the subcriticality in dollar units, because the sensitivities of the Bell factor to cross-sections are cancelled between the area ratio and subcriticality.*

## I. INTRODUCTION

Accelerator-driven system (ADS) [1] is a system proposed as a nuclear transmutation technology to reduce half-life of High-Level Waste (HLW) and TRans Uranium (TRU) waste. This system couples a subcritical core with a spallation neutron source. To maintain a safe operation in ADS, the core should be kept in the subcritical state.

The area ratio method, or the Sjöstrand method [2] is one of the subcriticality measurement techniques to monitor the subcritical state of a core. The absolute value of subcriticality can be obtained by analyzing the temporal variation of neutron density in a core due to the periodic injection of neutron pulses. This method is applicable to the ADS if an accelerator driven neutron source can produce periodic neutron pulses.

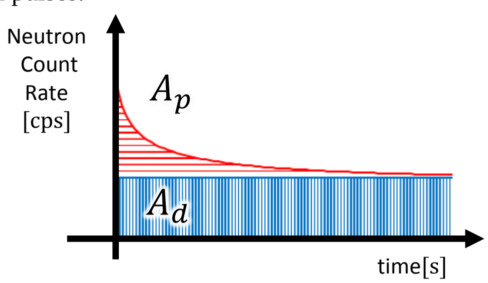


Fig. 1. Concept of the Sjöstrand method.

In practice, the subcriticality is measured by the temporal variation of neutron count rate, detected by a neutron detector in a system. As shown in Fig. 1, the time integral of measured neutron counts can be divided into two areas: One is the area due to prompt neutrons $A_p$, and another is the area due to delayed neutrons $A_d$. The ratio of $A_p$ to $A_d$, which is called as "the area ratio", yields a value of the subcriticality in dollar units:

$$\frac{A_p}{A_d} \approx \frac{-\rho}{\beta_{\mathrm{eff}}}, \qquad (1)$$

where $\rho$ is reactivity and the absolute value of negative reactivity $-\rho$ means subcriticality; $\beta_{\mathrm{eff}}$ is effective delayed neutron fraction. From here, we call the left and right hand sides of the equation as the area ratio "$AR$," and subcriticality in dollar units "$-\rho_{\$}$", respectively.

Equation (1) is approximately derived using the point kinetics model. In an actual subcritical core, the measured area ratio is not necessarily equal to the exact value of subcriticality in dollar units, due to distortion by spatial higher-order modes. In addition, the energy dependence of the neutron flux and the detector affects the area ratio [3]. Hence, in the actual measurement, the value of the area ratio is corrected. One of the correction methods is the use of Bell and Glasstone correction factor (the Bell factor) [4], obtained by a numerical calculation. The Bell factor $f$ is defined by the ratio of the subcriticality to the area ratio at a detector position $\vec{r}_d$ as follows:

$$f(\vec{r}_d) \equiv -\rho_{\$}/AR(\vec{r}_d). \qquad (2)$$

By multiplying the measured area ratio by the Bell factor $f$, effects of the spatial higher-order mode and energy dependence in the area ratio can be corrected.

Recently, we have been investigating the uncertainty of the Bell factor due to cross-section covariance. Previously, we quantified uncertainty of the Bell factor in a thermal core system, which is a simplified model of the Kyoto University Critical Assembly (KUCA) loaded with highly enriched uranium fuel [5]. In this study, we quantified the uncertainty in a fast reactor core based on the ADS design with minor actinide (MA) fuel proposed by JAEA [6].

In the previous uncertainty quantification of the Bell factor, the following two-step analyses were carried out: (1) Covariance evaluation of few-group homogenized cross-section through lattice calculations and (2) Uncertainty quantification of the Bell factor and subcriticality in core analysis. However, in the previous method, there is a problem: the larger number of collapsed energy groups requires higher calculation cost of covariance evaluation using the General Perturbation Theory (GPT) in the lattice calculation. This is because one GPT calculation is required for each collapsed/homogenized cross-section. In this study, to make the calculation scheme more efficient, we propose an improved method: Utilization of random sampling method [7].

## II. THEORY

### 1. Bell factor

Firstly, let us explain the calculation method of the Bell factor. When neutron flux $\phi(\vec{r},t,E)$ at position $\vec{r}$, time $t$ and energy $E$ is numerically evaluated by a calculation code, neutron count $A$ of a detector response is calculated [8] as

$$A(\vec{r}_d) = \iiint \Sigma_d(\vec{r},E)\phi(\vec{r},t,E)\, dV\, dt\, dE, \quad (3)$$

where $\Sigma_d(\vec{r},E)$ is the macroscopic detection cross-section, $\vec{r}_d$ is the detector position. The neutron flux must be calculated by solving a fixed source problem, where the pulsed neutron source is given as the external neutron source. Now, let us consider the time integral of the periodic flux $\phi(\vec{r},t,E)$ over the period of neutron pulse, $\tilde{\phi}(\vec{r},E)$. This integral value is equivalent to time integral of neutron flux due to a single pulse over the infinite time. Consequently, the integral flux $\tilde{\phi}(\vec{r},E)$ can be calculated by the time-independent neutron transport equation, and the neutron counts $A$ can be expressed as follows:

$$A(\vec{r}_d) = \iint \Sigma_d(\vec{r},E)\tilde{\phi}(\vec{r},E)\, dV\, dE. \quad (4)$$

The value of area ratio is calculated by Eq. (5) since $A = A_p + A_d$.

$$\begin{aligned} AR(\vec{r}_d) &= \frac{A_p(\vec{r}_d)}{A_d(\vec{r}_d)} = \frac{A_p(\vec{r}_d)}{A(\vec{r}_d) - A_p(\vec{r}_d)} \\ &= \frac{\iint \Sigma_d(\vec{r},E)\tilde{\phi}_p(\vec{r},E)\, dV\, dE}{\iint \Sigma_d(\vec{r},E)\{\tilde{\phi}(\vec{r},E) - \tilde{\phi}_p(\vec{r},E)\}\, dV\, dE}, \end{aligned} \quad (5)$$

where $\tilde{\phi}_p(\vec{r},E)$ is integral flux calculated by considering contribution only from prompt neutrons.

### 2. Effective delayed neutron fraction

In order to calculate the subcriticality in dollar units, additional calculations of the effective neutron multiplication factor $k_{\text{eff}}$ and the effective delayed neutron fraction $\beta_{\text{eff}}$ are necessary. These values can be obtained from the $k_{\text{eff}}$-eigenvalue calculation, not from a fixed source calculation. If the total number of delayed neutron precursor groups is six, $\beta_{\text{eff}}$ is calculated using the fundamental mode of forward and adjoint fluxes $\varphi(\vec{r},E)$ and $\varphi^\dagger(\vec{r},E)$ as follows [8]:

$$\beta_{\text{eff}} = \sum_{i=1}^{6} \frac{\int I_{d,i}^\dagger(\vec{r})\, F_{d,i}(\vec{r})\, dV}{\int I^\dagger(\vec{r})\, F(\vec{r})\, dV}, \quad (6)$$

where variables $F$, $F_{d,i}$, $I^\dagger$ and $I_{d,i}^\dagger$ are respectively defined as:

$$F(\vec{r}) = \int \nu\Sigma_f(\vec{r},E)\, \varphi(\vec{r},E)\, dE, \quad (7)$$

$$F_{d,i}(\vec{r}) = \int \nu_{d,i}\Sigma_f(\vec{r},E)\, \varphi(\vec{r},E)\, dE, \quad (8)$$

$$I^\dagger(\vec{r}) = \int \chi(\vec{r},E)\, \varphi^\dagger(\vec{r},E)\, dE, \quad (9)$$

$$I_{d,i}^\dagger(\vec{r}) = \int \chi_{d,i}(\vec{r},E)\, \varphi^\dagger(\vec{r},E)\, dE. \quad (10)$$

### 3. Uncertainty quantification using random sampling

In order to easily treat larger number of energy groups in core analysis, the random sampling method is used in the present uncertainty quantification. Figure 2 shows the whole uncertainty quantification scheme.

In a conventional two-step (lattice-core) core analysis, few-group homogenized cross-sections are firstly evaluated by energy collapsing and spatial homogenization in the lattice calculation. After that, the core calculation using the few-group homogenized cross-sections is carried out.

In the previous study, the uncertainty quantification scheme included (1) covariance evaluation among few-group homogenized cross-section by the GPT in the lattice calculation and (2) uncertainty quantification of the Bell factor and subcriticality in core analysis. In step (1), a GPT calculation is required for each few-group homogenized cross-section. This requires large calculation cost when larger number of collapsed energy groups is taken into account to accurately analyze core calculation.

In this study, to solve this problem, the covariance evaluation for few-group homogenized cross-sections is not carried out. Instead, the random sampling of microscopic cross-sections for the lattice calculation is performed followed by the two-step core analysis.

In the core calculation, evaluation of the target parameters, such as the Bell factor and subcriticality, is performed using each randomly perturbed few-group homogenized cross-section sample.

Finally, the uncertainty of target parameters is estimated from the statistical processing of the target parameter samples obtained by core calculations using randomly perturbed cross-sections.

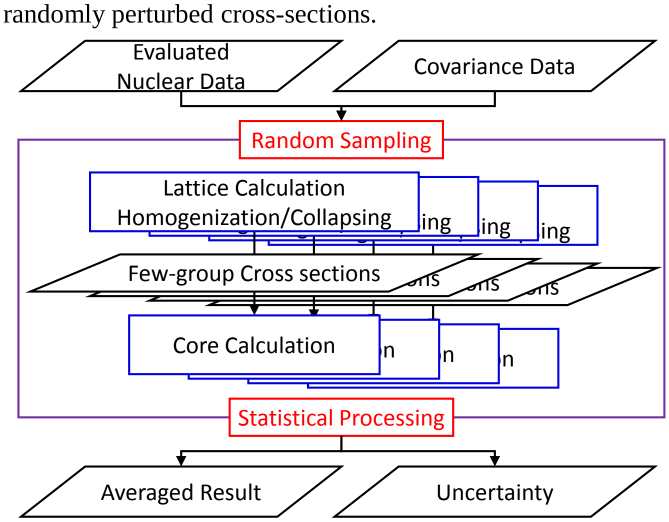


Fig. 2. Calculation scheme for uncertainty analysis.

In the new method using the random sampling method, the calculation cost for uncertainty quantification does not depend on the number of collapsed energy groups. Therefore, the uncertainty quantification can be performed with a certain number of samples regardless of the number of collapsed energy groups. It should be noted that accuracy of estimated uncertainty depends on the total number of samples $N$ used in the random sampling method. For a parameter $X$ of which probability distribution is well approximated by the normal distribution, the relative statistical error $S_{\sigma X}$ of the evaluated standard deviation $\sigma_X$ is estimated by:

$$\frac{S_{\sigma X}}{\sigma_X} \approx \frac{1}{\sqrt{2(N-1)}}. \tag{11}$$

For example, if $N = 1000$, the relative statistical error will be around 2 %.

### 4. Sensitivity Analysis

To verify the results of random sampling, and to analyze the cause of uncertainty, we performed the sensitivity analysis using direct method in the core calculation. The sensitivity analysis is based on a simple forward difference quotient as follows:

$$\frac{\Sigma_i}{X}\frac{\partial X}{\partial \Sigma_i} \approx \frac{\Sigma_i}{X(\Sigma_i)}\frac{X(\Sigma_i + \Delta\Sigma_i) - X(\Sigma_i)}{\Delta\Sigma_i}, \tag{12}$$

where the left-hand side of the equation is the relative sensitivity of a neutronics parameter $X$ to a nuclear data $\Sigma_i$ in the core calculation, and $\Delta\Sigma_i$ is the finite difference of $\Sigma_i$.

Using the relative sensitivity coefficients obtained by Eq. (12), the variance $\sigma_X^2$ of the parameter $X$ is estimated by the "sandwich formula":

$$\left(\frac{\sigma_X}{X}\right)^2 = \sum_i \sum_j \left\{ \left(\frac{\Sigma_i}{X}\frac{\partial X}{\partial \Sigma_i}\right) \frac{\mathrm{cov}(\Sigma_i, \Sigma_j)}{\Sigma_i \cdot \Sigma_j} \left(\frac{\Sigma_j}{X}\frac{\partial X}{\partial \Sigma_j}\right) \right\}, \tag{13}$$

where $\mathrm{cov}(\Sigma_i, \Sigma_j)$ means the covariance between two nuclear data $\Sigma_i$ and $\Sigma_j$. To quantify uncertainty in the core calculation using this method, the covariance of few-group homogenized cross-sections must be evaluated from the samples of them.

## III. CALCULATION GEOMETRY AND CONDITION

### 1. Target System

In this study, uncertainty quantification is carried out for one-dimensional cylinder geometry, in order to investigate magnitude and spatial distribution of uncertainty in a subcriticality measurement of MA loaded ADS. This system is a simplified model based on a cylindrical model of an ADS design proposed by JAEA [6]. This system is a fast reactor system loaded with a MA fuel and a Lead-Bismuth Eutectic (LBE) spallation target in the center of the core.

### 2. Lattice Calculation

In the evaluation of few-group homogenized cross-section and covariance using the random sampling method, SCALE 6.2.1 system with the V7-238 cross-section library and the 56groupcov7.1 covariance library [9] are used. The random sampling of cross-sections is performed by SCALE 6.2.1/Sampler module. The number of sample is 1000, which makes about 2 % of statistical error on the evaluated standard deviation.

The spatial homogenization and energy collapsing ("lattice calculation") of cross-section is carried out considering the whole core of the two-dimensional cylinder ADS design. By the neutron transport calculation of SCALE 6.2.1/NEWT module, the cross-sections are collapsed into 7 groups and homogenized into 4 regions, i.e., LBE (LBE Target + LBE Buffer), Core (MA core + Gas plenum), Reflector and Shield. However, the SCALE 6.2.1/NEWT transport calculation code cannot directly handle cylindrical r-z geometry. Therefore, a coordinate transformation to Cartesian geometry is performed conserving the average chord length in each region. The transformed geometry for homogenization and collapsing calculation is shown in Fig. 3.

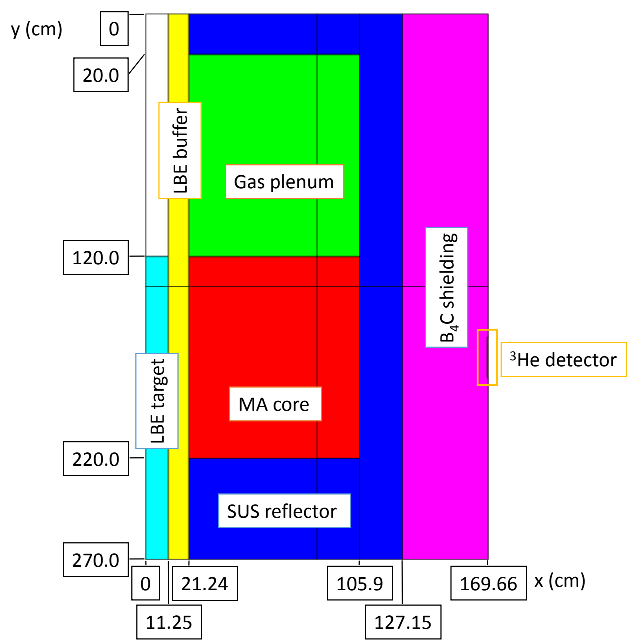


Fig. 3. Calculation geometry for homogenization and collapsing calculation.

Here, the left boundary condition is reflective, and the other boundary conditions are vacuum. To save calculation time, mesh division for this calculation is coarse, i.e. 2 × 2 for the whole system. This coarse mesh calculation produces a few % of systematic error in the 7 group homogenized cross-sections relative to the fine mesh calculation of 5 cm × 5 cm width. But, because the neutron flux is converged, it is expected that this discretization error does not have a large influence on the estimated uncertainty using the random sampling method. The material composition is set as same as the original ADS system. The group structure for energy collapsing is shown in Table I.

Table I. 7-group energy structure

| Group | Upper energy | Corresponding 238 groups |
|---|---|---|
| 1 | 20 MeV | 1-17 |
| 2 | 1.36 MeV | 18-38 |
| 3 | 400 keV | 39-45 |
| 4 | 85.0 keV | 46-57 |
| 5 | 9.50 keV | 58-71 |
| 6 | 683 eV | 72-85 |
| 7 | 100 eV | 86-238 |
| | 0.0001 eV | |

Using the NEWT module, 1000 samples of perturbed cross-sections obtained from the Sampler module are homogenized and collapsed, and each 7 group homogenized cross-section is used in the successive core calculation for uncertainty quantification by random sampling method. In addition, using these 1000 samples of 7 group homogenized cross-sections, the standard deviation and covariance of 7 group homogenized cross-sections are evaluated for the uncertainty quantification by sensitivity analysis.

### 3. Core Calculation

The uncertainty quantification of target neutronics characteristics, such as the subcriticality and the Bell factor, is carried out in the "core calculation". The core geometry for the core calculation is approximated by a one-dimensional cylindrical geometry. This geometry is a simplified model on the basis of ADS design by JAEA. For this simplification, the r-z model of ADS design is transformed into 1D cylinder to conserve the average chord length. In addition, the volume of MA core region is expanded to become $k_{\mathrm{eff}} = 0.97$, which is the design target of ADS in JAEA. The obtained 1D core geometry is shown in Fig. 4.

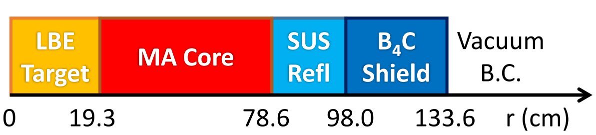


Fig. 4. Calculation geometry for core calculation.

A neutron source is located at the edge mesh of LBE Target region. For simplicity, the intensity of the neutron source is 1.0 neutrons/cm$^3$/sec for 1$^{st}$ energy group, and zero for other groups. Here, the absolute value of neutron source does not affect the value of area ratio, but the relative energy spectrum is important to calculate the area ratio.

The detector in the calculation is modeled as a point $^3$He detector. The absolute value of $\Sigma_d$ and that of flux does not affect the ratio of neutron count, but the relative energy dependence of $\Sigma_d$ is also meaningful. For simplicity, the 7 group cross-section of $\Sigma_d$ is obtained by collapsing the absorption cross-section of $^3$He mixture located at the edge of $B_4C$ shielding as shown in Fig. 3.

In this system, (1) the subcriticality in dollar units is evaluated by $k_{\mathrm{eff}}$-eigenvalue calculations without external neutron source, and the spatial dependencies of (2) the area ratio are evaluated by fixed source calculations with various neutron detector positions while the location of neutron source is fixed. The spatial dependencies of (3) the Bell factor is evaluated using the result of (1) and (2). In these calculations, we used an in-house one-dimensional diffusion code to evaluate the subcriticality, the area ratio and the Bell factor. This code solves the conventional finite-differential equations by Eigen library [10] for C++.

The uncertainty of (1) the subcriticality in dollar units, (2) the area ratio and (3) the Bell factor are evaluated in two methods: (a) the random sampling using 1000 samples of the 7 group homogenized cross-sections, and (b) the sensitivity analysis using the unperturbed data and the covariance of 7 group homogenized cross-sections. In the case of (b) the sensitivity analysis, the perturbation size for the finite difference $\Delta\Sigma_i$ is 1 % of the cross-section $\Sigma_i$. The uncertainty of (3) the Bell factor is directly evaluated using the samples of the Bell factor or Eqs. (12) and (13), not by the propagation of the uncertainty of (1) the subcriticality in dollar units and (2) the area ratio.

## IV. RESULTS

### 1. The spatial distribution of Bell factor and uncertainty

As a result of uncertainty quantification using random sampling method, the effective neutron multiplication factor is evaluated as $k_{\mathrm{eff}} = 0.970 \pm 0.011$ (1.1 %), the effective delayed neutron fraction as $\beta_{\mathrm{eff}} = 0.00188 \pm 0.00032$ (17 %), and the subcriticality as $-\rho_{\$} = 17.0 \pm 7.2$ [\$] (43 %), respectively. Here, the uncertainty is one sigma of standard deviation obtained by the random sampling, and the number in parenthesis means the relative standard deviation. Figure 5 shows the value of Bell factor and its relative standard deviation at each detector position due to cross-section uncertainty evaluated by random sampling method.

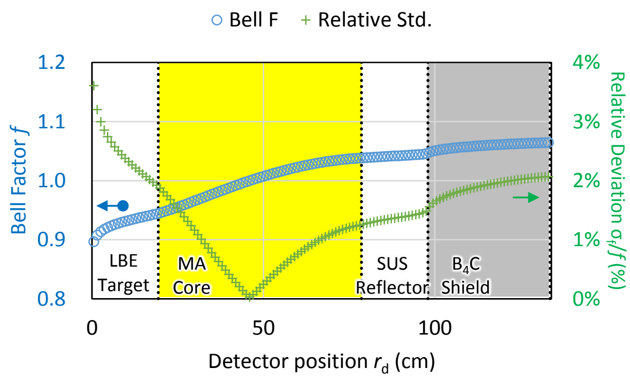


Fig. 5. The Bell factor and its relative standard deviation.

According to Fig. 5, the value of Bell factor exceeds unity when the detector is located in the reflector or the shielding region. The Bell factor is $f = 1.064 \pm 0.022$ (2.1%) at the end of shielding where the uncertainty is the largest in the reflector and shielding region. The Bell factor is $f = 0.897 \pm 0.032$ (3.6%) at the center of the core region where the uncertainty is the largest in all positions. The results shows the uncertainty of the Bell factor falls in the range below 4 %, which is smaller than that of subcriticality in dollar units, for all detector positions. Uncertainty of the Bell factor becomes smaller when the value of the Bell factor is close to unity, i.e., the difference between the area ratio and the subcriticality in dollar units is small.

## 2. Sensitivity and Correlation Analysis

First, Fig. 6 shows the results of sensitivity analysis for the subcriticality in dollar units to 7 group homogenized cross-sections of core region. Only the results of core region are shown in this paper, because the sensitivity coefficients to cross-sections of LBE, reflector and absorber regions are much smaller than that of the core region.

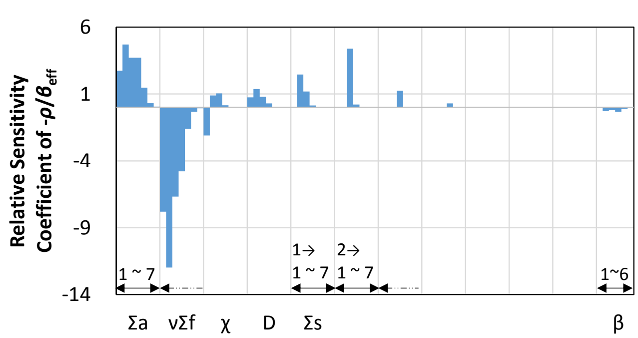


Fig. 6. Relative sensitivity of $-\rho_{\$}$ to 7g cross-sections of the core region

In Fig. 6, the horizontal axis shows the cross-sections: $\Sigma_a$ is absorption, $\nu\Sigma_f$ is production, $\chi$ is fission spectrum, $D$ is diffusion coefficient and $\Sigma_s$ is scattering from 1st to 7th energy group, and $\beta$ is delayed neutron fraction from 1st to 6th group. Similarly, Fig. 7 shows the relative sensitivity of the area ratio of the detector position at 56 cm. In addition, Fig. 8 shows the relative sensitivity of the area ratio at 46 cm, where the Bell factor is the closest to unity and the uncertainty of the Bell factor is the smallest in this calculation.

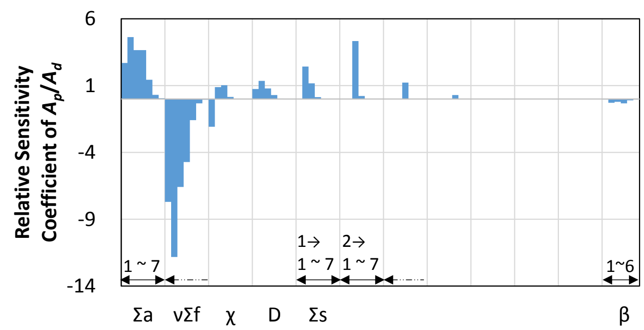


Fig. 7. Relative sensitivity of $AR$ at 56 cm ($f = 1.0171 \pm 0.0058$) to 7g cross-sections of the core region

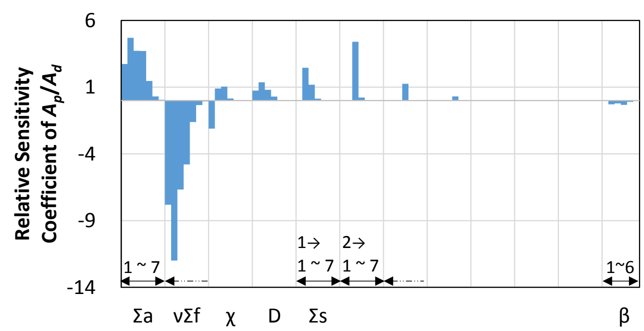


Fig. 8. Relative sensitivity of $AR$ at 46 cm ($f = 0.99974 \pm 0.00030$) to 7g cross-sections of the core region

From Figs 6-8, the relative sensitivities of the area ratio have similar values to that of the subcriticality in dollar units $-\rho_{\$}$.

Next, the results of the sensitivity analysis of Bell factor at 56 and 46 cm are shown in Figs. 9 and 10, respectively.

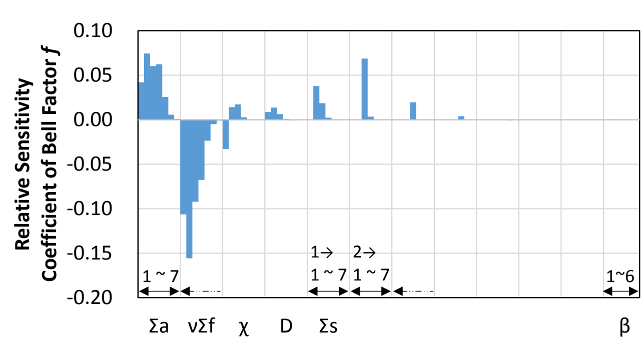


Fig. 9. Relative sensitivity of Bell factor at 56 cm ($f = 1.0171 \pm 0.0058$) to 7g cross-sections of the core region

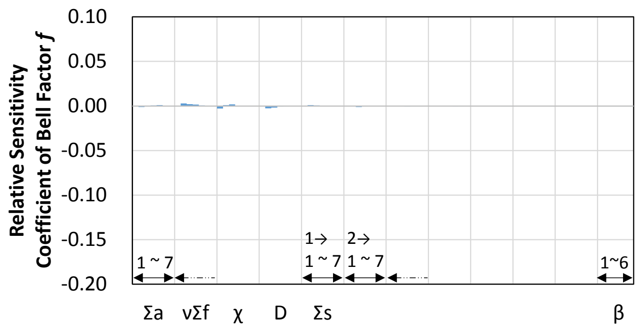


Fig. 10. Relative sensitivity of Bell factor at 46 cm ($f = 0.99974 \pm 0.00030$) to 7g cross-sections of the core region

From Figs.9 and 10, the relative sensitivity of the Bell factor is significantly different between these two positions: The relative sensitivity at 46 cm, where the Bell factor is almost unity, is much smaller than that at 56 cm. In addition, from the results of sensitivity analysis for other positions, the closer to unity the Bell factor is, the smaller the relative sensitivity of Bell factor becomes.

Because the Bell factor $f$ is defined as the ratio of the subcriticality and the area ratio by Eq. (2), the sensitivity of Bell factor to a nuclear data $\Sigma_i$ can be obtained using the sensitivity of those values by following equation:

$$\frac{\Sigma_i}{f}\frac{\partial f}{\partial \Sigma_i} = \frac{\Sigma_i}{-\rho_\$}\frac{\partial(-\rho_\$)}{\partial \Sigma_i} - \frac{\Sigma_i}{AR}\frac{\partial AR}{\partial \Sigma_i}. \quad (14)$$

This equation shows the relative sensitivity of Bell factor is given by the difference between that of the subcriticality and that of the area ratio. The sensitivity of Bell factor calculated by Eq. (14) using that of the area ratio and the subcriticality in Figs 6-8 is consistent with the results of Eq. (12) in Figs 9-10.

When the detector is set at a position where the area ratio is just equal to the subcriticality in dollar units, i.e. Bell factor $f$ is unity. For such a detector position, Eq. (1) is satisfied, and by differentiating Eq. (1), the sensitivity of $-\rho_\$$ is the same as that of $AR$:

$$\frac{\partial(-\rho_\$)}{\partial \Sigma_i} = \frac{\partial AR}{\partial \Sigma_i}. \quad (15)$$

In this case, by substituting Eq. (1) and Eq. (15) into Eq. (14), the relative sensitivity of the Bell factor approaches zero. In addition, as mentioned before in Figs. 6-7, the sensitivity of $-\rho_\$$is almost the same as that of $AR$ for other detector positions; thus the relative sensitivity of the Bell factor on Eq. (14) is small as shown in Fig. 9. Based on the sandwich formula, Eq. (13), this fact resulted in the small uncertainty of Bell factor as shown in Fig. 5.

## V. CONCLUSIONS

We investigated the uncertainty quantification of the Bell factor, which is spatial correction factor in a subcriticality measurement using the Sjöstrand method, due to the uncertainty in cross-section data.

In this study, the uncertainty of the Bell factor is evaluated by the random sampling method for a one-dimensional cylinder system of a simplified ADS using 7 group diffusion calculations. The result shows the uncertainty of the Bell factor due to cross-section uncertainty is smaller than that of the subcriticality in dollar units. In addition, the uncertainty of the Bell factor tends to become smaller when the area ratio and subcriticality in dollar units becomes closer.

The sensitivity analysis of the Bell factor and related parameters to 7 group cross-sections is also performed. As a result, the sensitivity coefficients of the area ratio are close to those of the subcriticality in dollar units. In addition, the closer the area ratio to the subcriticality in dollar units is, the smaller the difference between the sensitivity coefficients of them are. Therefore, the sensitivity coefficient of the Bell factor and thus its uncertainty are cancelled out.

## REFERENCES


1. T. SASA, "Studies on Accelerator-driven System in JAEA and Transmutation Experimental Facility Program," ISOLDE Seminar, November 1st, 2013, https://indico.cern.ch/event/280019/ (2013).
2. N. G. SJÖSTRAND, "Measurements on a Subcritical Reactor Using a Pulsed Neutron Source," *Arkiv för Fysik*, **11**(13), 233–246 (1956).
3. A. TALAMO, Y. GOHAR, Y. CAO, Z.ZHONG, H. KIYAVITSKAYA, V.BOURNOS, Y. FOKOV, C. ROUTKOVSKAYA, "Impact of the neutron detector choice on Bell and Glasstone spatial correction factor for subcriticality measurement," *Nucl. Instrum. Methods Phys. Res. Sect. A*, **668**, 71–82 (2012).
4. A. TALAMO and Y. GOHAR, "Deterministic and Monte Carlo Modeling and Analyses of YALINA-Thermal Subcritical Assembly," ANL-NE-10/17, Argonne National Laboratory (2010).
5. T. KIMURA, T. ENDO, A. YAMAMOTO, "Uncertainty Quantification of Spatial Correction Factor for Sjöstrand Method due to Cross-section Data," *Proc. 2016 ANS Winter Meeting*, Las Vegas, Nevada, November 6-10, 2016, American Nuclear Society (2016) (CD-ROM).
6. H. IWAMOTO, K. NISHIHARA, R. KATANO, M. FUKUSHIMA and K. TSUJIMOTO, "Effect of Experiments Using Transmutation Physics Experimental Facility on the Reduction of Uncertainties in Reactor Physics Parameters of an Accelerator-Driven System," JAEA-Research 2014-033, Japan Atomic Energy Agency (2014).

7. A. YAMAMOTO, K. KINOSHITA, T. WATANABE, T. ENDO, Y. KODAMA, Y. OHOKA, T. USHIO, H. NAGANO, "Uncertainty Quantification of LWR Core Characteristics Using Random Sampling Method," *Nucl. Sci. Eng.*, **181**(2), 160-174 (2015). (CD-ROM).
8. G. I. BELL and S. GLASSTONE, *Nuclear Reactor Theory*, p.551, Van Nostrand Reinhold, New York (1970).
9. "SCALE Code System," ORNL/TM-2005/39, Version 6.2.1, Oak Ridge National Laboratory (2016).
10. Gaël Guennebaud, "Eigen: a C++ template library for linear algebra and related numerical algorithms," *Bibliothèques pour le calcul scientifique*, Palaiseau, France, May 15th, 2013, Association Aristote (2013).